MEASUREMENTS OF GAMMA-RAY PRODUCTION CROSS SECTIONS FOR SHIELDING MATERIALS OF SPACE NUCLEAR SYSTEMS+

V. J. Orphan, Joseph John, and C. G. Hoot

Gulf Radiation Technology
A Division of Gulf Energy & Environment Systems Incorporated

Measurements of secondary gamma-ray production from neutron interactions have been made over the entire energy range (thermal to 16 MeV) of interest in shielding applications. A LINAC pulsed neutron source having a continuous distribution of neutron energies is used in conjunction with high-resolution Ge(Li) gamma-ray spectrometers and the time-of-flight technique. The two-parameter data (gamma-ray energy vs neutron energy) are obtained using a computer-controlled data acquisition system. Two facilities are used in the measurements. A 16-meter facility is used to measure gamma rays from resonant capture of neutrons up to 100 KeV. Gamma production cross sections from (n,xy) reactions are measured up to 16 MeV using a 50-meter facility.

The epithermal capture gamma-ray yields for both resolved gamma-ray lines and continuum have been measured from thermal energies to 100 KeV for natural tungsten and ^{238}U, two important candidate shield materials in SNAP reactor systems. Data are presented to illustrate the variation of epithermal capture gamma-ray yields with neutron energy. In the resolved resonsance region, the total observed radiated energy was within ± 15% of the known binding energy. The gamma-ray production cross sections from (n, xy) reactions have been measured for Fe and Al from the threshold energies for in-elastic scattering to ∿16 MeV. Typical Fe and Al cross sections obtained with high-neutron energy resolution (∿1% at 1 MeV) and averaged over broad neutron-energy groups are presented and compared with previous cross-section determinations made using monoenergetic neutron sources.

1. INTRODUCTION

The design of space nuclear systems, both for electric power generation and for propulsion, requires an accurate knowledge of secondary gamma-ray production cross sections over a wide neutron energy range. The necessity of optimizing shield designs for minimum weight places particularly strong demands on the precision of these cross sections. There are, in general, two different types of gamma-ray production data required: (1) gamma-ray yields from the radiative capture,(n,y) reactions, of neutrons in the energy range, thermal to about 100 keV, and (2) gamma-ray production cross sections for (n, xy) reactions of neutrons in the range, threshold for inelastic scattering to about 16 MeV. The relative importance of these two types of data in a particular space application depends, of course, on such related considerations as the material, the incident neutron flux spectrum, the geometrical configuration, the dose constraint, etc.

There is a general lack of secondary gamma-ray production data adequate for use in the analysis of radiation transport in space nuclear systems. The numerous requests (ref. 1) for this type of data testify to the current widespread deficiency.

This paper describes a program of measurements carried out at the Gulf Radiation Technology LINAC in order to provide urgently needed gamma-ray production data of the two types mentioned above. A technique for measuring epithermal capture gamma-ray yields is briefly described and typical results are shown for tungsten and depleted uranium, two important candidate shield materials for space electric power systems. Also, a method of measuring gamma-ray production cross sections for (n, xy) reactions up to 16 MeV is discussed. Representative results are shown for iron and aluminum (important structural and shield materials in space nuclear systems, such as NERVA) and these are compared with previous results in order to illustrate the advantages of the LINAC technique for obtaining gamma-ray production data.

2. EPITHERMAL CAPTURE GAMMA-RAY YIELDS

Shields consisting of a heavy metal such as ^{238}U, W, Pb or Ta, (for gamma-ray shielding) and LiH (for neutron shielding) are being considered for use in both the SNAP and thermionic electric power systems. The total capture gamma-ray yield from the heavy metal in such shields depends on both the capture cross section and the gamma-ray spectrum, i.e., the distribution of capture gamma rays as a function of gamma-ray energy. It has been shown (ref. 2) that the dose penetrating these shields is quite sensitive to the variation of epithermal capture gamma-ray spectra with neutron energy. Nevertheless, a lack of epithermal capture data has made necessary the use of thermal capture spectra in many shielding calculations even though it is known that a significant fraction of the captures take place at epithermal energies. In this section, measurements of the epithermal capture gamma-ray spectra for ^{238}U and W using a pulsed LINAC neutron source are described. Furthermore, typical results are given to illustrate the variation of spectra with neutron energy and to compare the contrast the ^{238}U and W data.

+ This work supported by the Defence Atomic Support Agency under Contract DASA 01-69-C-0083 and the U.S. Atomic Energy Commission under Subcontract No. 3032 with Union Carbine Corporation.

2.1 EXPERIMENTAL TECHNIQUE

A schematic of the capture gamma-ray facility (ref. 3) is shown in fig. 1. A LINAC target, consisting of a water-cooled tungsten alloy (fansteel) converter surrounded by a 15.3-cm-diam right circular cylinder of depleted uranium, is used to produce a pulsed source of neutrons having a continuous distribution of energies. Neutrons are moderated by a 2.54-cm-thick piece of polyethylene placed around the target. The neutrons travel down a 16-meter evacuated flight path and impinge on a 15.2-cm-diam capture sample placed at 45° to the neutron beam. The capture gamma rays from the sample are detected by a Ge(Li)-NaI spectrometer mounted on a movable carriage as shown in Fig. 1. Measurements are usually made at an angle of 90° with respect to the incident neutron beam. The energy of the neutron producing the capture gamma ray is determined by measuring the time interval between the LINAC burst and the gamma-ray event in the spectrometer; i.e., the time-of-flight (TOF) technique. An example of a TOF spectrum is shown in Fig. 2 for ^{238}U. The number of gamma rays detected by the spectrometer (counts/channel) is plotted against neutron flight time (channel number) and clearly illustrates the lower energy capture resonances in ^{238}U.

The Ge(Li)-NaI spectrometer may be simultaneously operated in three modes: (1) as a single Ge(Li) detector, (2) Compton suppression spectrometer, (3) three-crystal pair spectrometer using a computer-controlled data acquisition system. Each counting event is suitably "tagged" before storage in the computer to identify the mode in which the event is detected. The Compton suppression mode is most useful for studying lower energy capture gamma-rays from 0.1 to 3 MeV. The pair spectrometer is used to detect higher energy gamma rays, above 1.5 MeV. The simplification afforded by the pair spectrometer is illustrated in Fig.3 which shows a comparison of the tungsten capture gamma-ray spectrum measured in the singles mode (upper spectrum) and in the pair mode (lower spectrum) for neutron energies between 2.5 and 6.0 eV. The Compton background, which increases sharply with decreasing gamma-ray energy in the singles spectrum is practically eliminated in the pair spectrum. The full-energy and single-escape peaks that complicate the analysis of the singles spectrum are totally absent in the pair spectrum. The peak-to-back-ground ratio at 5164 keV is improved by a factor of 16. This simplification of complex spectra made possible by the nearly ideal single-line response of the pair spectrometer facilitates the unfolding of these spectra to obtain the intensities of continuum gamma-rays. Previous epithermal capture measurements which concentrated on the intensities of the discrete lines are of limited usefulness in shielding calculations since they do not include the large fraction (up to 95 percent) of the total capture gamma-ray intensity that appears as continuum for many elements. The spectrometer used in the present investigation makes possible the measurement of this important continuum contribution.

The experimental data are accumulated in two-parameter form (gamma-ray energy and neutron TOF) using an on-line computer. This two-parameter data is sorted off-line into gamma-ray pulse height spectra for the capture of neutrons with energies between two specified limits. Four capture gamma-ray spectra from ^{238}U measured in the pair spectrometer mode are shown in Fig. 4. The spectra are for "thermal" capture (E_n = 0.02 to 0.5 eV) and for capture in the 6.67-, 21.0- and 36.7-eV resonances. The neutron energy limits used to cover these and other low energy resonance are shown in the ^{238}U(n,y) TOF spectrum given in Fig. 2. Note in Fig. 4 the sharp variation with neutron energy of the intensities of discrete lines, especially the doublet (unresolved in our spectra) with lines at 3982 and 3991 keV and a triplet (also unresolved) with components at 4052, 4059, and 4068 keV (refs. 4,5).

2.2 DATA REDUCTION

The spectra obtained in the pair spectrometer and Compton suppression modes were unfolded (ref. 6) to remove the effects of the spectrometer response and the results were used to determine gamma-ray intensities for capture in ^{238}U. The relative number of captures in the sample as a function of incident neutron energy was calculated from the known capture cross section and resonsance parameters for ^{238}U and the measured flux shape. Detailed corrections were made for finite sample effects such as neutron attenuation, neutron multiple scattering, gamma-ray self-absorption, etc. The capture gamma-ray intensities were normalized to a previous determination (ref. 4) of the intensities of discrete lines from thermal neutron capture. Details of the data analysis and complete results for ^{238}U have been previously reported (ref. 7).

2.3 TYPICAL RESULTS FOR ^{238}U AND W

The gamma-ray intensities for capture in ^{238}U have been determined for 15 neutron energy groups spanning the range 5 eV to 100 keV. The intensities were determined for gamma-ray energy bins about 240-keV wide and include the contribution of both discrete and continuum gamma rays above about 1 MeV. Figure 5 shows, in histogram form, typical results for four energy groups. In addition to the intensities (lower curve in each plot), Fig. 5 shows the radiated energy for each gamma-ray energy bin. The calculated uncertainties are indicated on each curve. The sum of the radiated energy gives a check on the accuracy of the results. For nine of the neutron energy groups, this sum agreed with the known binding energy within $\pm$ 15%. Most of the other groups showed disagreements of the order of 20% and in these cases the results were renormalized to 97% of the binding energy, the mean value obtained from results for the first four strong resonsances in ^{238}U for gamma-ray energies greater than 900 keV.

Epithermal capture gamma-ray spectra have also been previously measured and reported (ref. 8) for natural tungsten. Results for tungsten have been reported for 10 neutron energy intervals spanning the range 1.5 eV to 100 keV. Capture gamma-ray intensities in photons/100 captures were grouped into 500-KeV gamma-ray energy bins over the energy range 1.0 to 7.5 MeV.

It is of interest to compare some of the epithermal capture gamma-ray spectra from tungsten and uranium since the shield designer often must choose between different heavy metals. Figure 6 shows a comparison of the capture gamma-ray yield distributions from depleted uranium and tungsten for two representative neutron energy intervals. The first interval spans the 6.67-eV ^{238}U resonance of the 7.65-eV ^{183}W resonance and the second interval, 0.5 keV to 1.0 keV, spans many closely spaced resonances in uranium and tungsten. As is illustrated in fig. 6, the tungsten and uranium capture gamma-ray yield distributions are quite different. Tungsten has a much harder gamma-ray spectrum for both neutron energy ranges primarily because the average neutron binding energy for natural tungsten is considerably higher than that of uranium. For instance for the 7.65-eV tungsten resonance the binding energy is 7.3 MeV while for the 6.67-eV ^{238}U resonance the binding energy is only 4.8 MeV. Note also that the magnitude of the difference in the capture gamma-ray spectra between tungsten and uranium depends on the neutron energy. The difference between the two spectra are seen in Fig. 6 to be significantly less for the 0.5 keV to 1 keV interval than for the intervals spanning the low energy resonance.

The large differences shown in this comparison demonstrate the need for the measurement of epithermal capture gamma-ray spectra for other important shield materials. In applications where a large fraction of the captures take place above thermal neutron energies, such data as described above for uranium and tungsten are essential for an accurate calculation of the secondary gamma-ray dose.

3. GAMMA-RAY PRODUCTION CROSS SECTIONS FOR (n,xy) REACTIONS

The use of moneonergetic neutron sources, usually produced with a Van de Graaff accelerator using the d-d reaction, to measure gamma-ray production cross sections results in good neutron energy resolution and accurate angular distribution studies. However, a systematic study of the energy dependence of these cross sections over a wide neutron energy range, which is required for accurate radiation transport calculations, is extremely time consuming. This is especially true if the cross section has sharp resonances which necessitate a monoenergetic measurement at many neutron energies in order to obtain the true average cross section. Furthermore, measurements with a Van de Graaff accelerator are increasingly difficult to interpret in the neutron energy range above 9 MeV, since neutrons from the d-d reaction are not monoenergetic because of deuteron breakup.

On the other hand, the use of a pulsed LINAC neutron source having a continuous distribution of energies allows gamma-ray production cross sections to be measured continuously over a wide neutron energy range in a single experimental run. The LINAC technique sacrifices neutron energy resolution to some extent but has the distinct advantage of providing a consistent set of average cross sections for a series of contiguous energy intervals spanning the entire neutron energy range of interest in most shielding calculations. Furthermore, when necessary, the neutron energy resolution of this technique as is illustrated in Fig. 11 can be made comparable or even better than that of Van de Graaff measurements.

3.1 EXPERIMENTAL TECHNIQUE

A facility for the measurement of (n,xy) cross sections using a LINAC has been described previously (ref.9). Consequently, the experimental arrangement, which is shown schematically in Fig. 7, is only briefly described in order to review the principal details of the technique. The Ta-Be target, shown in Fig. 7, produces a copious yield of high energy neutrons with a minimum of gamma flash (bremsstrahlung from electrons striking the Ta converter). The neutrons traverse a 51-meter evacuated flight path and impinge on a ring-shaped scattering sample (48.3 cm o.d. and 27.9 cm i.d.) in which gamma-ray producing reactions occur. The energy of the gamma rays is measured with an 80-cm^3 Ge(Li) detector located on the flight path axis near the sample and shadow shielded from source neutrons and gamma rays. The corresponding neutron energy is obtained by recording the time when a gamma-ray event is detected in the Ge(Li) detector relative to the LINAC pulse, i.e., by the time-of-flight technique. These two-parameter data are accumulated using an on-line computer in a manner similar to that used in the measurement of epithermal capture spectra. The Ge(Li) detector is positioned at an angle of approximately 125° to the incident neutron beam. Since the second Legendre polynomial is zero at 125°, this choice minimizes the effect of gamma-ray anisotrophy on the determination of the integrated gamma-ray production cross section from a measurement at a single angle.

The 80-cm^3(Ge(Li) detector* is sectioned to operate as a total absorption (or DUODE) spectrometer (ref. 10) as well as an ordinary Ge(Li) detector. Spectra for the two different operating modes of the detector are stored simultaneously using the same tagging features of the data-accumulation code discussed earlier in Section 2.1 for the Ge(Li)-NaI spectrometer. The principal advantages of using a total absorption spectrometer to study gamma-ray spectra from (n,xy) reactions are illustrated in Fig. 8 which shows the gamma-ray spectrum from the ^{nat}Fe(n,n'y) reaction for neutrons in the energy range, 0.8 MeV to 1.5 MeV. The upper spectrum was measured with the Ge(Li) detector in the singles mode while the lower spectrum was simultaneously measured with the detector in the DUODE mode. The improved response function of the DUODE mode of operation results in a significant decrease in the Compton distribution and it facilitates the unfolding of complex spectral data to obtain the intensity of continuum gamma rays. The principal background peak in the singles mode results from internal conversion decay of the 695-keV level in 72Ge excited by neutrons scattered into the Ge(Li) detector. Note that this background peak is almost completely absent in the DUODE spectrum. Thus, use of the DUODE has the added

* Purchased from Princeton Gamma-Tech. Inc., Princeton, New Jersey.

advantage of eliminating a principal background line nearly always present in (n,n'y) studies using Ge(Li) detectors.

The two-parameter data (gamma-ray energy, neutron energy) are usually sorted to obtain gamma-ray spectra (for both operating modes of the spectrometer) corresponding to selected neutron energy intervals spanning the energy range from the threshold for (n,xy) reactions to about 16 MeV. Gamma-ray spectra below about 3.5 MeV gamma-ray energy from the ^{nat}Fe (n,n'y) reaction measured with the Ge(Li) detector operated in the DUODE mode are given in Fig. 9. The 27 spectra which cover the neutron energy range, 0.85 MeV to 16.6 MeV, illustrate the variation of the gamma-ray spectra from (n,xy) reactions with neutron energy. Note, for example, that as the neutron energy increases, the spectra become more complex with more high energy gamma rays and an indication of a significant continuum contribution.

3.2 CROSS-SECTION DETERMINATIONS

Broad-group gamma-ray production cross sections are obtained as a function of neutron energy for discrete lines by determining the peak areas in gamma-ray spectra such as those shown in Fig. 9 for the DUODE mode or in similar spectra obtained simultaneously in the singles mode with better counting statistics. Cross sections are derived from the peak areas corrected for the variation of the neutron flux with energy, for Ge(Li) detector effiency, for neutron attenuation and multiple scattering in the sample, for gamma-ray self-absorption in the sample, for scattered neutron background, and the deadtime of the electronics'. These data-reduction procedures have been described in detail elsewhere (ref.11).

High-resolution gamma-ray production cross sections may be obtained by sorting the two-parameter data in a manner which is the reverse of that described above for obtaining broad group data. Namely, TOF spectra are generated corresponding to a narrow pulse height (gamma-ray energy interval). The procedure is illustrated in Fig. 10 which shows the gamma-ray spectrum from (n,xy) reactions in iron andthe TOF spectra generated for a gamma-ray energy interval (815 KeV $\leq E_y \leq$ 873 keV) encompassing the 847-keV gamma ray from the first excited state in ^{56}Fe (spectrum A) and for an interval (902 keV $\leq E_y \leq$ 960 keV) at slightly higher gamma-ray energy (spectrum B). Spectrum B provides a good approximation of the Compton background contribution from higher energy gamma rays since this background is reasonably uniform over the two gamma-ray energy intervals specified above. These data, accumulated in a 14-hour LINAC run, have more than adequate counting statistics to determine considerable structure in the 847-keV gamma-ray production cross section, especially just above the threshold energy. The neutron energy resolution is about 1% at 1 MeV and is limited primarily by the use of a 20-nsec LINAC pulse width, However, the resolution of the present measurement can be improved by almost a factor of seven by using the available minimum pulse width of 3 nsec. The difference between TOF spectrum A and spectrum B corrected as described above for broad group cross sections, has been used to determine a high resolution gamma-ray production cross section for the 847-keV gamma-ray from $^{56}Fe(n,n'y)^{56}Fe$.

3.3 HIGH-RESOLUTION CROSS SECTIONS FOR Fe and Al

Figure 11 shows the integrated high resolution cross section for the 847-keV gamma-ray obtained from $4\pi\frac{d\sigma}{d\omega}(125°)$ with a small correction ($\sim$10% just above threshold, less than 2% above 3 MeV) for anistrophy of the gamma rays. The neutron energy resolution is represented by the FWHM of the triangle shown at various energies. The error bars shown for every fifth point include only the error due to counting statistics. There is an additional estimated systematic uncertainty (primarily from the absolute flux measurement) of about 10%.

These high resolution gamma-ray production cross-section measurements are not as suitable for radiation transport calculations as are broad group average cross sections. However, the determination of high resolution cross sections facilitates a comparison between continuous values obtained with the LINAC source and those obtained with a monoenergetic neutron source at widely spaced energies. This is especially true when the cross section has a great deal of structure.

Some previous determinations of the 847-keV gamma-ray production cross section using a monoenergetic neutron source are shown for comparison in Fig. 11. The present results are significantly lower (on the average about 23%) in the energy range, $5.6 \leq E_n \leq 7.8$ MeV than the measurements of Drake et al. (ref. 12), although there is good agreement at 4.0 MeV. There is good agreement up to 4.5 MeV with the values calculated from the (n, n') cross sections by Kinney and Perey (ref. 13). The present data are in close agreement with the recent data of Dickens and Perey (ref. 14) over the range $5.35 \leq E_n \leq 8.0$ MeV but are about 20% lower than their data at 9 MeV. There is good agreement with the Texas Nuclear Corp. (TNC) data except at 14.8 MeV where their results are about a factor of two higher. However, the present data are in excellent agreement with the 14-MeV measurements of Benetsky and Frank (ref. 16) and Clayeux and Grenier (ref. 17).

The present measurement provides the gamma-ray production cross section over a wide energy range $0.86 \leq E_n \leq 16$ MeV and fills in important energy gaps, especially in the 9- to 14- MeV region where no previous measurements exist. Also, the LINAC technique is capable of resolving serious discrepancies between different measurements. This is particularly true when these discrepancies are primarily a result of sharp structure in the cross section. This situation is very well illustrated by the 847-keV gamma-ray production cross section for Fe. Figure 12 shows various monoenergetic measurements of this cross section as reported in BNL-325 (ref. 18). Note that there is nearly a factor of two discrepancy between the high and low values in the energy range shown. These large differences are primarily caused by systematic differences and by sharp structure resulting in a great sensitivity of the measured cross-section values in these Van de Graaff experiments to small uncertainties

in the beam energy and resolution. The dark stars in Fig. 12 are the present high-resolution results averaged over ∿ 0.5 MeV wide intervals. The present data are somewhat higher than the recommended curve in BNL-325 and do not indicate a fall-off around 4.5 MeV.

High-resolution cross sections have also been determined for several strong lines from the $^{27}Al(n,n'y)^{27}Al$ reaction. Figure 13 shows the gamma-ray production cross section for the 1013-keV gamma ray. Note that even though this cross section is about a factof of 5 smaller than the 847-keV Fe cross section,the counting statistics are quite adequate for these data, which were accumulated in less than 14 hours. In the region just above threshold (up to 2.2 MeV) one can compare the gamma-ray production cross section to (n,n') cross-section measurements since the 1013-keV level in ^{27}Al decays predominantly by gamma-ray emission to the ground state (ref. 19). There is good agreement with the (n, n') cross-section measurements below 1.5 MeV of Chien and Smith (ref. 20). At higher energies there is agreement with Day's value (ref.21) at 2.6 MeV and Hosoe and Susuki's value (ref. 22) near 3 MeV. In addition, there is fairly good agreement with the TNC measurements (ref. 15) between 3.6 and 4.6 MeV and the measurements of Chung et al. (ref. 23) at 3.5 MeV. As for the Fe data, there is good agreement with the measurements of Dickens (ref. 24) between 5.35 MeV and 8.5 MeV and 20 to 30% lower values than the data of Drake et al. (ref. 12) at 6.0 and 7.7 MeV. However, the present results are in close agreement with the 4-MeV value of Drake et al. In the vicinity of 14 MeV the present results lie between recent measurements at 14.1 MeV (ref. 17) and 15 MeV (ref. 25).

3.4 BROAD GROUP CROSS SECTIONS FOR Fe AND Al

Differential gamma-ray production cross sections at 125° have been determined for the principal gamma rays from (n, xy) reactions in Fe and Al. Broad group average cross sections were determinedfor 20 neutron energy groups spanning the range $0.86 \leq E_n \leq 16.7$ MeV. Typical examples of the results are given in fig. 14 for Fe and fig. 15 for Al.

Figure 14 shows plots of the cross sections for the 1408-1412-keV doublet, the 1811-keV line and the 2599-2604-keV doublet compared to several previous Van de Graaff measurements. In general, the present results are in very good agreement with the TNC data (ref. 15), the measurements of Dickens (ref.14), and two measurements (refs. 17,26) near 14 MeV. The 1408-keV and 1811-keV cross sections are lower than the measurements of Dickens above about 8 MeV. The dip in the cross section for the 1408-1412 doublet near 12 MeV is a consequence of the threshold of the $^{56}Fe(n,2ny)^{55}Fe$ reaction at 12.85 MeV, above which there is a sharp increase in the yield of the 1412-keV gamma ray.

Figure 15 shows the differential cross section for three Al gamma rays, the 1809-,2210-, and 3001-keV lines. Comparison with existing published data is also given with fair agreement. The main disagreements are with the 14.8 MeV measurements from the TNC compilation (ref. 15) which are also higher than other 14-MeV measurements shown, and with the points of Drake et al. (ref. 12), at 6 and 7.5 MeV for the 2210-keV line.

3.5 CONTRIBUTION OF CONTINUUM GAMMA RAYS

In some cases the gamma-ray production cross sections measured for discrete lines represent only a fraction of the total gamma-ray production cross section. The present results for Fe at the higher neutron energies help illustrate this point. An examination of the Fe spectra reveals a significant number of weak gamma rays whose individual gamma-ray production cross sections are too small to determine accurately but whose collective sum amounts to a significant fraction of the total gamma-ray production cross section. For instance, Drake et al. (ref. 12), have unfolded their gamma-ray spectra (measured with a NaI detector) from (n, xy) reactions in iron at 6.0 MeV and 7.5 MeV to obtain the total gamma-ray production cross section. They obtain total gamma-ray production cross sections of 3.9 b at 6.0 MeV and 4.7 b at 7.5 MeV. The total gamma-ray production cross section for 27 lines obtained in our measurement for the interval $6.03 \leq E_n \leq 7.54$ MeV is 2.2 b. This is roughly half of the total gamma-ray production cross section measured in this energy region by Drake et al., (4.3 b, the average of the 6.0 MeV and 7.5 MeV values). Thus, it is very important that the gamma-ray production cross section of the many weak lines be accounted for.

Our data are currently being unfolded in order to obtain the cross section for these weak gamma-ray lines and continuum gamma rays. Figure 16 shows the results of a preliminary unfolding using the MAZE1 code (ref. 6), of the gamma-ray spectrum Ge(Li) detector operated in singles mode) from $^{nat}Fe(n,xy)$ reactions of neutrons in the range, $6.03 \leq E_n \leq 7.54$ MeV. The gamma-ray spectrum was corrected for scattered-neutron background (about a 20% correction) and compressed by a factor of 18 prior to unfolding. The unfolded spectrum is shown in fig. 16 up to about 5 MeV gamma-ray energy along with a comparison between the original spectral data and a refolded spectrum generated from the unfolded spectrum and the detector response matrix. Note that there is good agreement between the refolded spectrum and the data. Furthermore, most of the structure in the unfolded spectrum can be associated with strong discrete gamma-ray lines from Fe. The unfolded spectrum of fig. 16 was used to calculate the gamma-ray production cross section of the sum of discrete and continuum gamma rays for 240-KeV wide gamma-ray energy intervals. A preliminary value for the total gamma-ray production cross section for the interval $6.0 \leq E_n \leq 7.5$ MeV is 4.4 b, which is in excellent agreement with the value (4.3 b) obtained from the masurements of Drake et al. Similar gamma-ray production cross sections will be determined for other neutron groups so that data which include continuum gamma rays will be available for 10 neutron energy groups spanning the range, 0.85 to 16.7 MeV.

4. SUMMARY

Techniques based on the use of a LINAC pulsed neutron source and a Ge(Li) gamma-ray detector have been described for the measurement of secondary gamma-ray production data continuously over the entire neutron energy range of interest in the shielding of space nuclear systems. Epithermal capture gamma-ray yields (including continuum gamma rays) were measured over the neutron energy range, thermal to 100 keV, and typical results for natural tungsten and depleted uranium were presented and contrasted. Measurements of gamma-ray production cross sections for (n, xy) reactions in the energy range 0.85 to 16 MeV were described. Some representative results for iron and aluminum were shown and compared to previous monoenergetic measurements in order to illustrate some of the principal advantages of the LINAC technique.

Epithermal capture gamma-ray spectra can be quite different from thermal spectra and can vary with neutron energy. Consequently, it is important that these spectra be measured for other candidate shield materials so that the designer can realistically evaluate the relative merits of each material. There are several major advantages of using the LINAC technique to study gamma-ray production cross sections for (n, xy) reactions.

1. Data are obtained in a single experimental run over a wide neutron energy range which includes the 9 to 14 MeV region where monoenergetic measurements are difficult.

2. The data are obtained in a form (namely, group-averaged cross sections) most suitable for use in radiation transport codes.

3. Coupled with Ge(Li) unfolding techniques, the use of a LINAC source provides an attractive means of obtaining the complete gamma-ray production cross section (discrete and continuum gamma rays) over the full neutron energy range of interest.

5. ACKNOWLEDGEMENTS

We are pleased to acknowledge many helpful discussions in the course of this work with V.C. Rogers, M. P. Fricke and C. A. Preskitt.

REFERENCES

1. Leona Stewart, H.T. Motz and M.S. Moore, "Compilation of Requests for Nuclear Cross Section Measurements", WASH-1144, Los Alamos Scientific Laboratory (Draft Copy; November 1969).

2. K. J. Yost and M. Solomito, "Sensitivity of Gamma-Ray Dose Calculations to the Energy Dependence of Gamma-Ray Production Cross Sections", Proc. Neutron Cross Sections and Technology Conference, NBS Special Publication 299, Vol. i, p. 53 (1968).

3. V. J. Orphan, C. G. Hoot, A. D. Carlson, Joseph John and J. R. Beyster, Nucl. Instr. and Methods 72, 254 (1969).

4. R.K. Sheline, W.N. Shelton, T. Udagawa, E.T. Jurney and H.T. Motz, Phys. Rev. 151, 1011 (1966).

5. D. L. Price, R. E. Chrien, O.A. Wasson, M.R. Bhat, M. Beer, M.A. Lone and R. Graves, Nucl. Phys. A121, 630 (1968).

6. M. Sperling, "Unfolding with the MAZE1 System, Volume 1" DASA Report Gulf-RT-10486, Gulf Radiation Technology (January 1971).

7. Joseph John and V.J. Orphan, "Gamma Rays from Resonant Capture of Neutrons in ^{238}U." Gulf General Atomic Report GA-10186 (June 15, 1970).

8. V. J. Orphan and Joseph John, "Intensities of Gamma Rays from the Radiative Capture in Natural Tungsten of Neutrons from 0.02 eV to 100 keV", Gulf General Atomic Incorporated Report GA-9121 (December 31, 1968).

9. V. J. Orphan, C.G. Hoot, A. D. Carlson, Joseph John and J. R. Beyster, Nucl. Instr. and Meth. 73, 12 (1969).

10. H. W. Kraner and R. L. Chase, "A Total Absorption Ge(Li) Gamma-Ray Spectrometer", IEEE Eleventh Scintillation and Semiconductor Counter Symposium, Feb. 1968.

11. V. J. Orphan, C. G. Hoot, and Joseph John, Nucl. Sci. Eng. 42, 352 (1970).

12. D. M. Drake, et al., Nucl. Sci. Eng. 40 294 (1970).

13. W. E. Kinney and F. G. Perey, Nucl. Sci. Eng. 40, 396 (1970).

14. J. K. Dickens and F. G. Perey, ORNL-4592, Oak Ridge National Laboratory (September 1970).

15. P. S. Buchanan, "A Compilation of Cross Sections and Angular Distributions of Gamma Rays Produced by Neutron Bombardment of Various Nuclei, "Report No. ORO 2791-28, Texas Nuclear Corporation (1969).

16. B.A. Benetsky and I. M. Frank, Proc. of International Conference on Nuclear Physics, Paris (1964) 817.

17. G. Clayeux and G. Grenier, "Spectres de Renvoi des Gammas Produits par des Neutrons de 14, 1 MeV", Report No. CEA-R-3807, CEN-Saclay (1969).

18. M. D. Goldberg, Neutron Cross Sections, BNL-325, 2nd Edition, Supplement No. 2, Feb. 1966.

19. J. H. Towle and W. B. Gilboy, Nucl. Phys. 39 , 300 (1962).

20. J. P. Chien and A. B. Smith, Nucl. Sci. Eng. 26, 500 (1966).

21. R. B. Day, Phys. Rev. 102 , 767 (1956).

22. Masano Hosoe and Shoji Suzuki, J. Phys. Soc. Japan 14, 699 (1959).

23. K. C. Chung, et al., Nucl. Phys. A115, 476 (1968).

24. J. K. Dickens, "Al(n,xy) Reactions for $5.3 \leq E_n \leq 9.0$ MeV," ORNL-TM-3284, Oak Ridge National Laboratory (January 18, 1971).

25. K. Nyberg, B. Jonsson, and I. Bergqvist, private communication.

26. F. C. Engesser and W. E. Thompson, J. Nucl. Energy 21, 487, (1967).

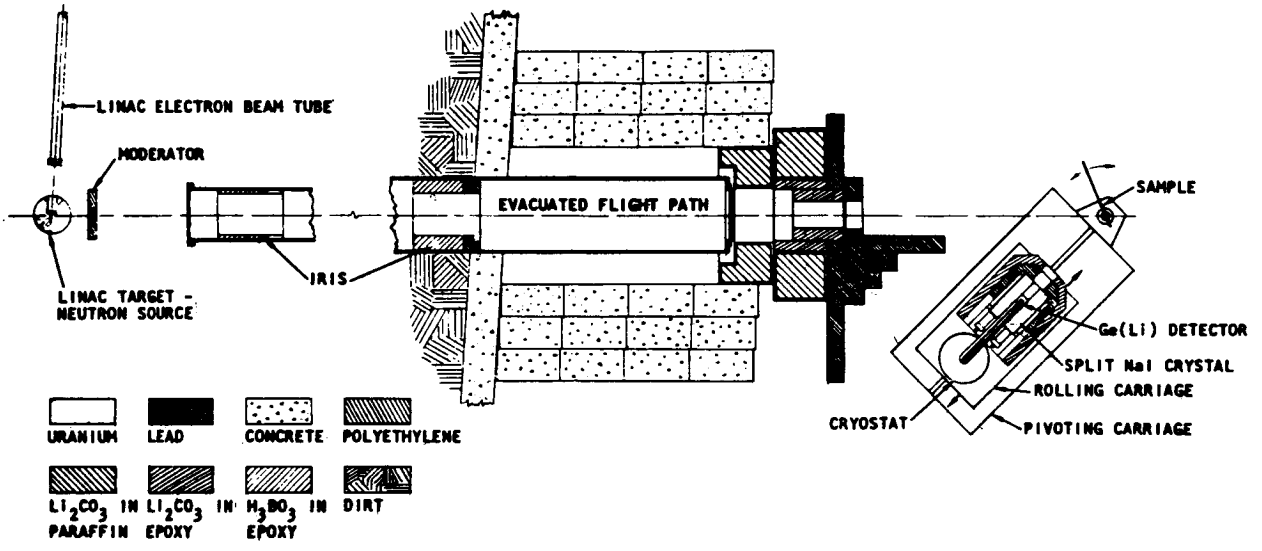

Figure 1. Schematic drawing of the capture gamma-ray facility. Details of the evacuated flight path, the beam defining collimators and the shielding arrangement are shown. To the right is the Ge(Li)-NaI(Tl) spectrometer with its shield and the movable carriage.

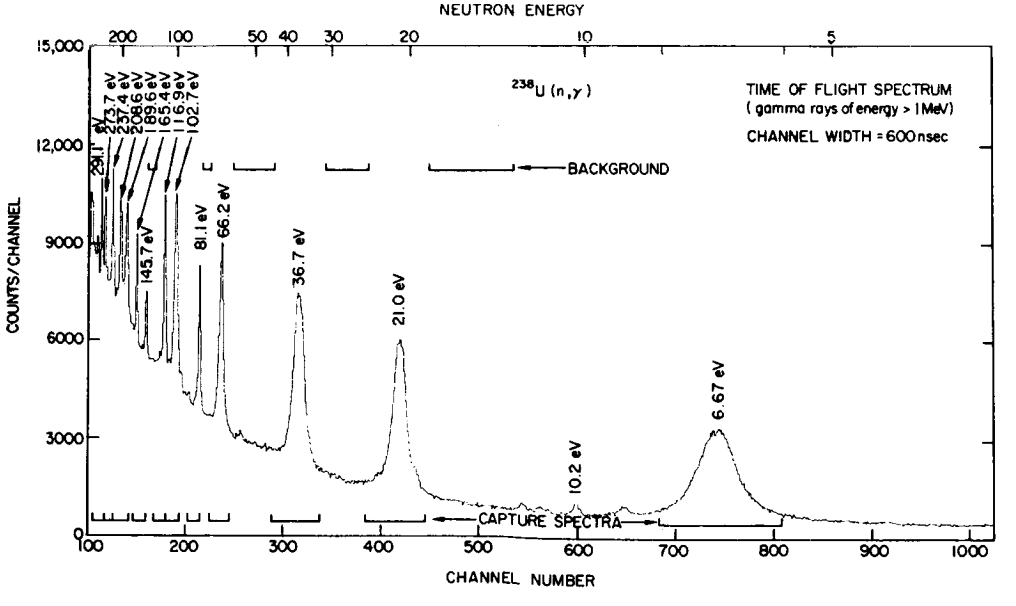

Figure 2. Neutron time-of-flight spectrum showing the low energy ^{238}U resonances. This spectrum was generated using only gamma rays that deposited at least 2 MeV in the Ge(Li) detector.

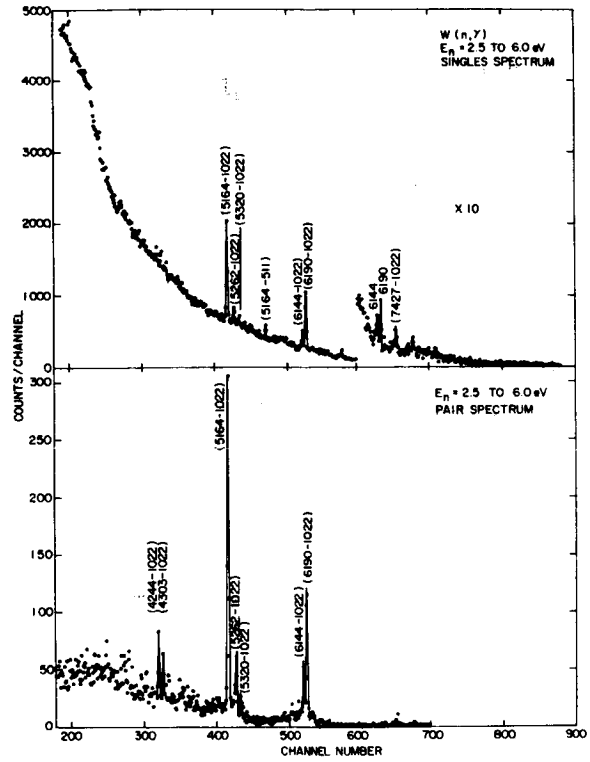

Figure 3. Comparison of capture gamma-ray spectra from tungsten obtained with singly-operated Ge(Li) detector (upper) and pair spectrometer (lower). Easy identification of peaks and high peak-to-background ratio in the pair spectrum is illustrated.

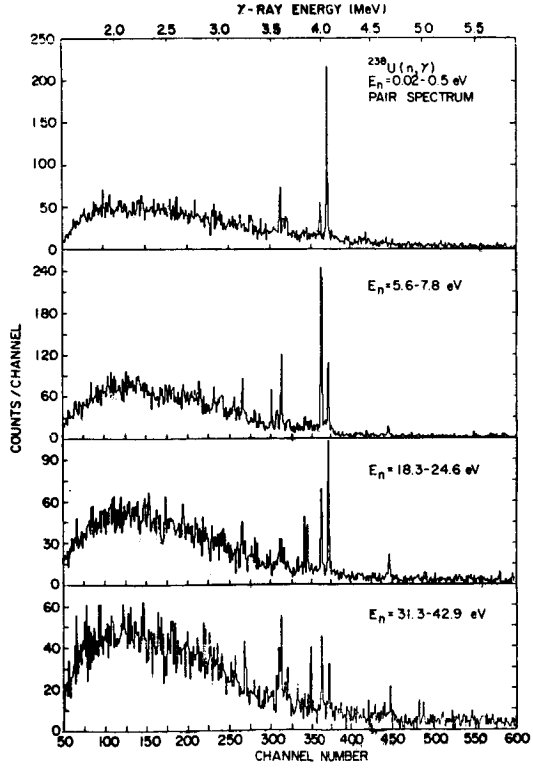

Figure 4. Comparison of measurements with the pair spectrometer of the ^{238}U capture spectra from neutrons in the energy ranges: 0.02-0.5 eV, 5.6-7.8 eV, 18.3-24.6 eV, and 31.3-42.9 eV.

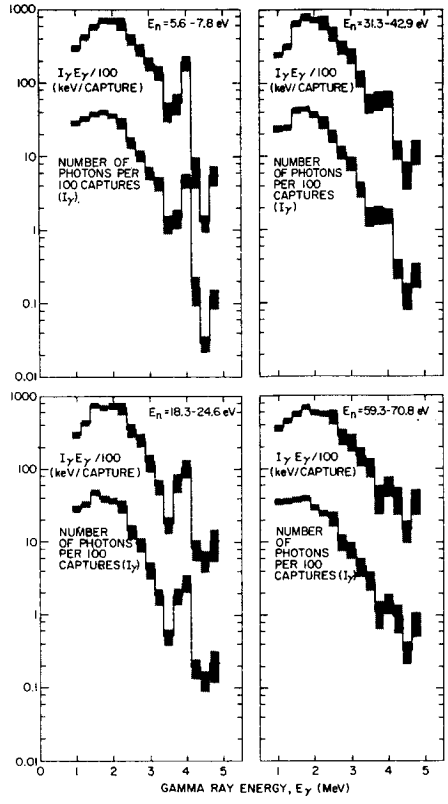

Figure 5. Intensities of capture gamma rays. The fractional radiated energy is also shown.

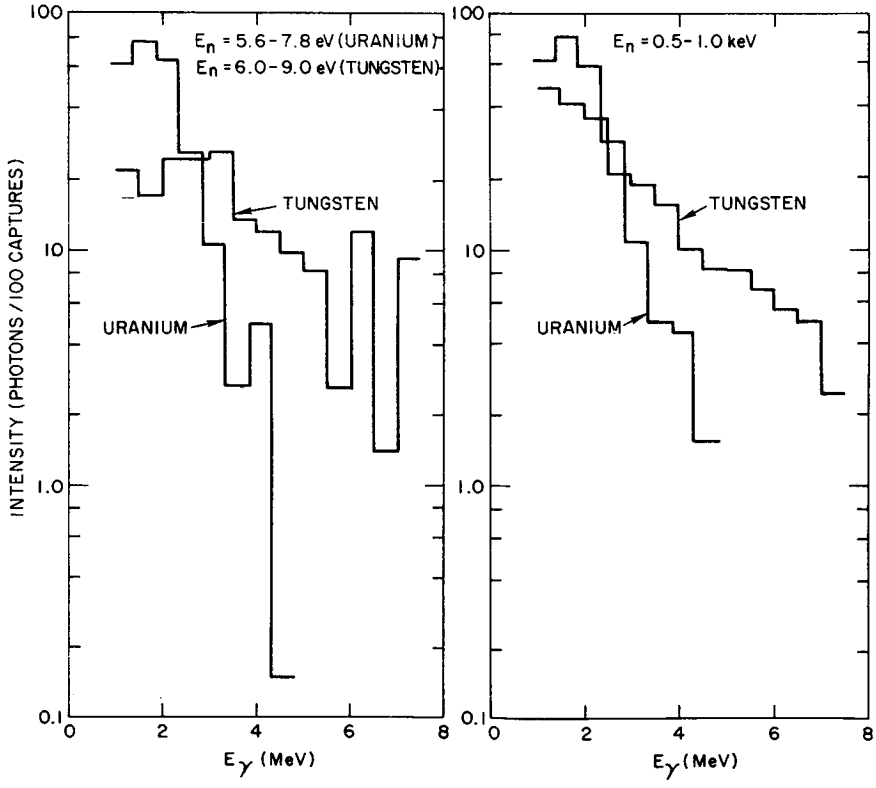

Figure 6. A comparison of capture gamma-ray intensities between uranium and tungsten for two neutron energy intervals.

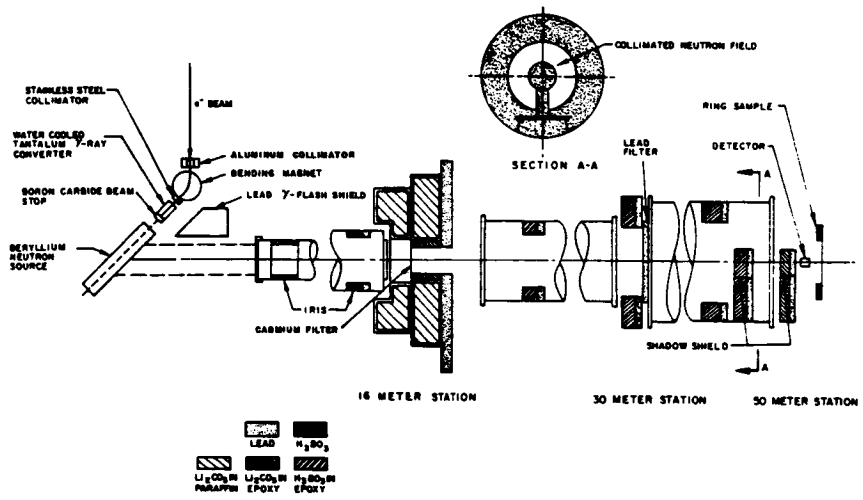

Figure 7. Schematic of the neutron flight path showing filters, irises, collimators, and shadow shields. The neutron source, the Ge(Li) detector, and the ring-shaped scattering sample are also shown.

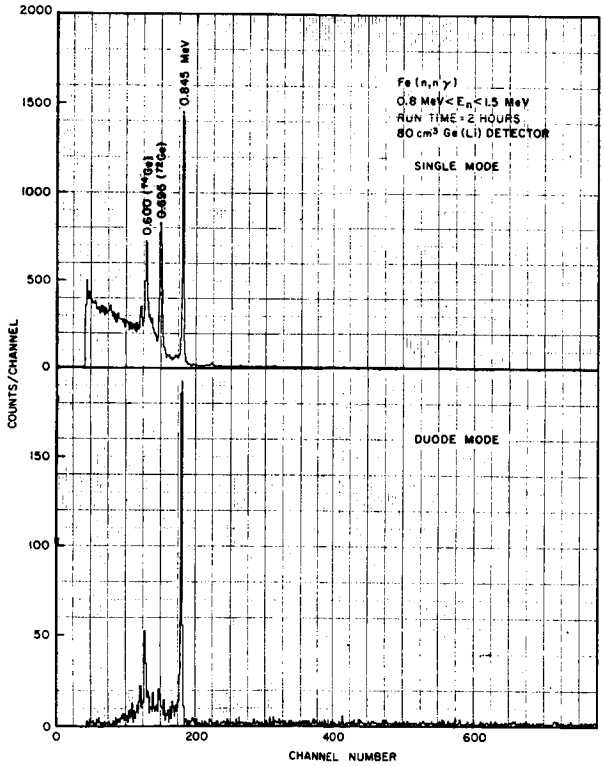

Figure 8. Gamma-ray spectrum from the $^{nat}Fe(n, n'\gamma)$ reaction for the neutron energy range, 0.8 MeV to 1.5 MeV, measured with the 80-cm^3 Ge(Li) detector in the singles mode (upper spectrum) and in the DUODE mode (lower spectrum).

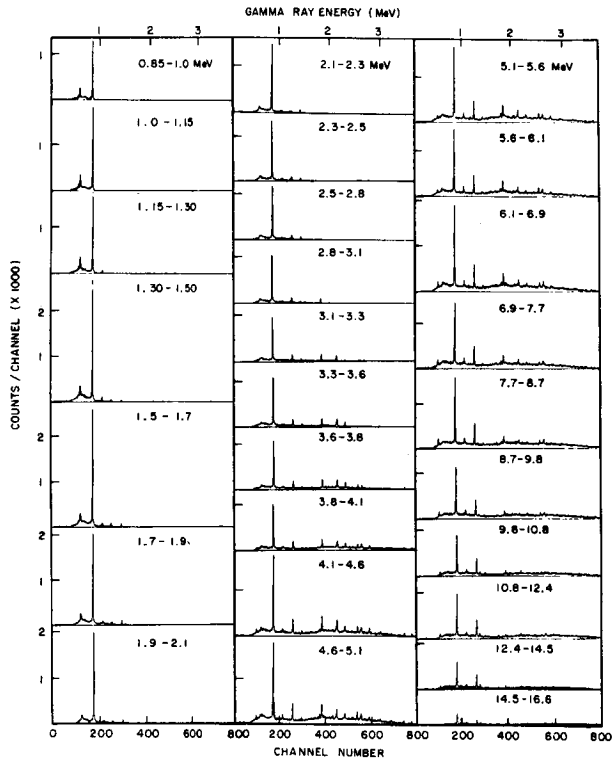

Figure 9. Gamma-ray spectra from Fe(n, xγ) reactions measured with the Ge(Li) detector operated in the DUODE mode. The variation of gamma-ray spectra with neutron energy is illustrated over the range, $0.85 \leq E_n \leq 16.6$ MeV.

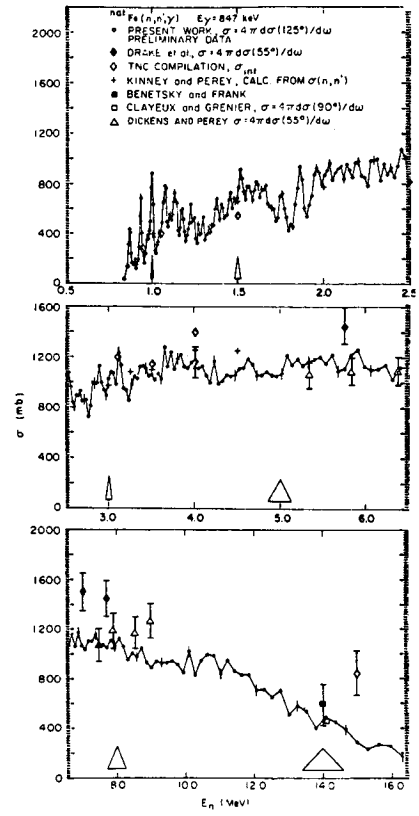

Figure 11. Gamma-ray production cross section for the 847-keV gamma ray from the $^{56}Fe(n, n'\gamma)$ reaction for neutron energy range, 0.86 MeV to 16 MeV.

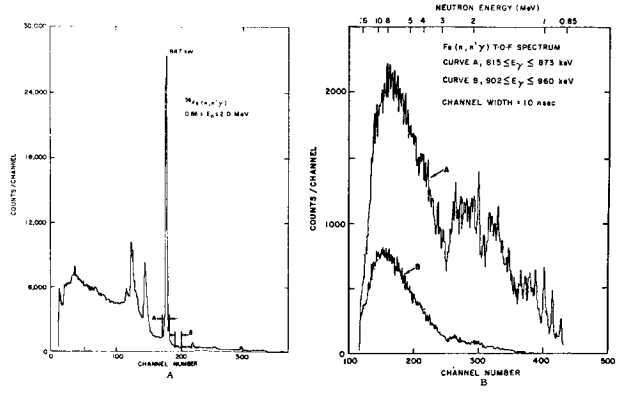

Figure 10. Gamma-ray spectrum from Fe(n, xγ) reactions (A) showing gamma-ray energy intervals for which the two time-of-flight spectra (B) were generated from two-parameter data.

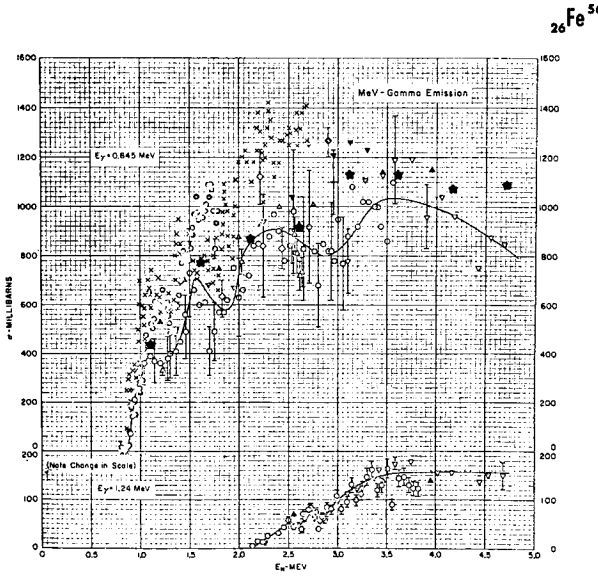

Figure 12. Comparison of present results averaged over ~ 0.5 MeV neutron energy intervals (indicated by "stars") with measurements compiled in BNL-325 (ref. 18).

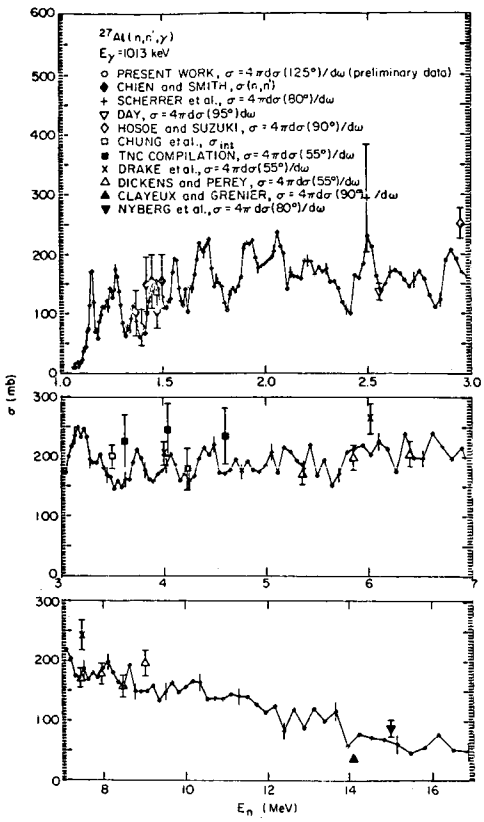

Figure 13. Gamma-ray production cross section for the 1013-keV gamma ray from the ^{27}Al(n, n'γ) reaction for neutron energy range 1.01 MeV to 16 MeV.

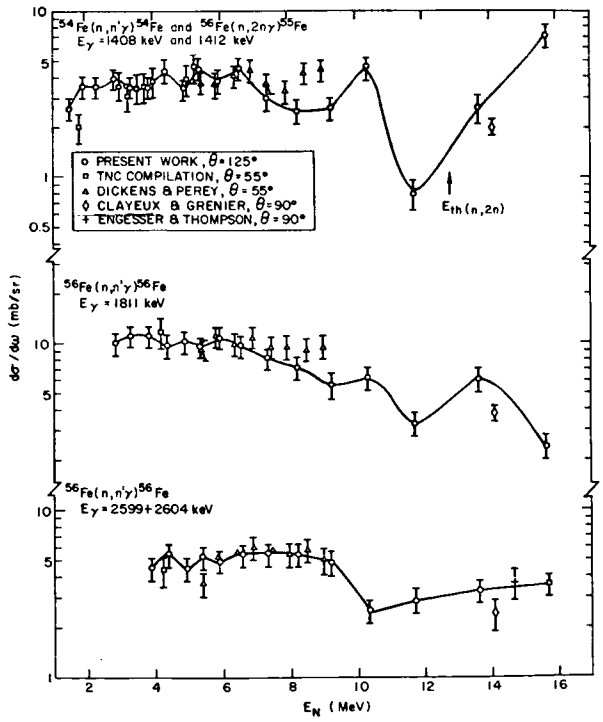

Figure 14. Differential gamma-ray production cross sections for neutron interactions with natural iron compared to previous data. The data points for the present work represent the average cross section over a neutron energy interval and are located at the midpoint of each interval. The solid line is simply a smooth curve connecting the present data points.

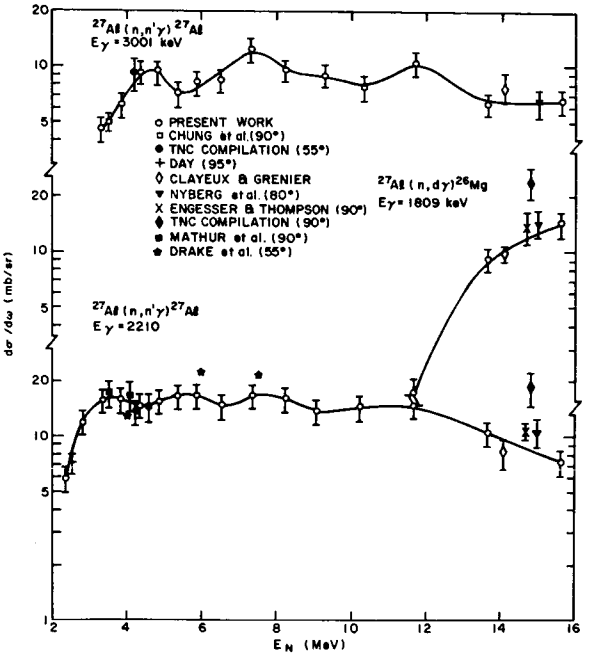

Figure 15. Differential gamma-ray production cross sections for neutron interactions with aluminum compared with previous data. The data points for the present work represent the average cross section over a neutron energy interval and are located at the midpoint of each interval. The solid line is simply a smooth curve connecting the present data points.

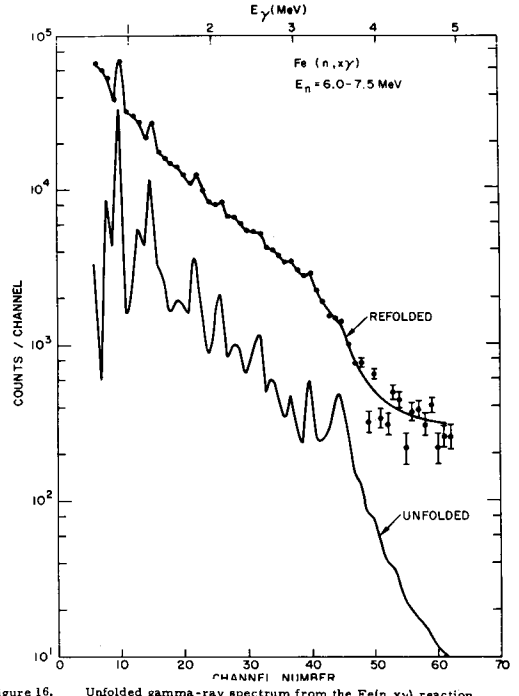

Figure 16. Unfolded gamma-ray spectrum from the Fe(n, xγ) reaction for neutrons in the neutron energy range 6.0 MeV to 7.5 MeV. The refolded spectrum is in good agreement with the original gamma-ray spectrum.